

Local density of states of II-VI ternary alloys in bulk and surfaces: an application to $\text{ZnSe}_{1-x}\text{Te}_x$

Daniel Olguín

*Departamento de Física, Centro de Investigación y de Estudios Avanzados del Instituto Politécnico Nacional
Apartado postal 14-740, 07300 México, D.F., Mexico*

Recibido el 8 de septiembre de 1998; aceptado el 8 de diciembre de 1998

Within a reformulated virtual crystal approximation, that takes into account the correct alloy dependence of the band gap value of the II-VI pseudobinary compounds, and using the surface Green's function matching method we calculate the bulk- and surface-projected local density of states of the $\text{ZnSe}_{1-x}\text{Te}_x$ alloy. We show that our approach gives correctly the band gap value and the electronic band structure of these ternary alloys.

Keywords: II-VI semiconductor alloy; local density of states

Mediante una reformulación a la aproximación del cristal virtual, con la cual describimos adecuadamente el cambio de la banda de energía prohibida como función de la concentración, y haciendo uso del método de empalme de la función de Green de superficie calculamos la densidad electrónica local de estados de la aleación $\text{ZnSe}_{1-x}\text{Te}_x$. Mostramos de esta manera la utilidad de nuestra aproximación.

Descriptores: Aleaciones de compuestos II-VI; densidad local de estados

PACS: 71.15.Fv; 71.22.+i; 73.20.At

1. Introduction

The study of the physics of surfaces, interfaces, quantum wells, and superlattices of semiconductors has been of interest in recent years [1–8]. This interest has not only focused on binary compounds but also on ternary and quaternary alloys [9–13].

In this work, and based on a corrected electronic band structure description of the binary compounds, we develop a method which serves as a basis to a clear and simple description of more complicated compounds and systems. A theoretical starting point, for the study of these systems, is an accurate description of the electronic band structure of the binary compound. This goal can be achieved using the empirical tight-binding method [14–19].

In previous work we have used the tight-binding method to study the band gap dependence with the alloy concentration in the ternary [12] and quaternary [13] alloys of the II-VI compounds. The tight-binding method in conjunction with the known surface Green's function matching method (SGFM) [20] was successfully used to study the electronic band structure of the (001) surfaces [19, 21], and derive the local density of electronic states (LDOS) at the surfaces and interfaces [22, 23].

In the II-VI ternary alloys we have shown that the tight-binding method, together with a reformulated virtual crystal approximation (VCA), gives full account of the non-linear dependence of the band gap value on the molar fraction [12]. Later this theory was also successfully applied to the II-VI quaternary alloys [13]. In this work we show an useful extension of our reformulation, namely, the calculation of the

LDOS in ternary alloys. One of the distinctive features of this scheme, in comparison with other schemes, is its efficiency and strong predictive power. The method, in comparison with the *ab initio* calculations that takes long time in supercomputer machines [24, 25], does not need supercomputer performance. We show that by modelling the ternary alloy as a pseudobinary compound we can use, in a straightforward way, the SFGM method and obtain, for example, the LDOS. In particular we have applied our model to study the LDOS of the (001)-surface of the $\text{ZnSe}_{1-x}\text{Te}_x$ ternary alloy. An application of our approach could be done straight out to study the electronic and optical properties of graded composition heterostructures. Sometimes, graded heterostructures are obtained due to unwanted diffusion of a chemical element, other times this effect is due to a deliberate design (for examples of these effects, in III-V quantum wells, see Refs. 1–4 in [26]). On the other hand, the compositionally graded interfaces appear to have some favorable effects. For example, $\text{Al}_x\text{Ga}_{1-x}\text{As}/\text{GaAs}$ quantum wells exhibit an enhanced quantum confined Stark effect, and the absorption in these systems is seen to decrease significantly with increased intermixing. These are favorable features for device applications, hence the interest in these systems. In recent work, theoretical study of these heterostructures have been done with the tight-binding method in the frame of the VCA [26, 27]. Although, the results obtained in that framework seems to be acceptable, it is possible that a refinement of these results could be attained using the approach described in the present work. The rest of the paper is organized as follows: In Sect. 2 we present the approach the method used. For completeness in Sect. 2.2 we give a brief description of the approach used

for the study of the ternary alloys. Section 3 shows our results and make a brief comment in reference to other calculations. We show explicitly how the results of our simple description compares to complex calculations. The conclusions are drawn in Sect. 4.

2. Method

2.1. The surface Green function method

To describe the surface of the ternary alloys, we will assume a pseudobinary compound. Within this picture, we can use the tight-binding Hamiltonians that we have proved to give correctly the band gap behaviour in the ternary and quaternary alloys. The use of the SGFM method allows us to do a detailed study of the surface. The SGFM method takes into account the perturbation caused by the surface or interface exactly, and we can use the bulk tight-binding parameters (TBP). The difference between the bulk parameters and the surface ones is taken into account through the matching of the Green's function [20, 28]. We use the method in the form cast by García-Moliner and Velasco [20]. They make use of the transfer matrix approach first introduced by Falicov and Yndurain [29]. This approach became very useful due to the quickly converging algorithms of López-Sancho *et al.* [30]. Following the suggestions of these authors, the algorithms for all the matrices needed to deal with these systems can be found in a straightforward way [30, 31].

The surface Green's function is found to be [20]

$$G_s^{-1} = (\omega I - H_{00}) - H_{01}T, \quad (1)$$

and the projected bulk Green's function, [20]

$$G_b^{-1} = G_s^{-1} - H_{01}^\dagger \tilde{T}, \quad (2)$$

where ω is the energy eigenvalue, H_{00} and H_{01} are the tight-binding Hamiltonians that describe the layered system. We adopt the customary description in terms of principal layers, and retain first nearest neighbors interactions between principal layers. It is well known that this method gives a correct electronic description of surfaces and interfaces [19, 21–23, 32].

It is customary to define the transfer matrices as

$$\begin{aligned} G_{k+1,p} &= TG_{kp}, & k \geq p \geq 0 \\ G_{i-1,j} &= \tilde{T}G_{ij}, & j \geq i \geq 0. \end{aligned} \quad (3)$$

These matrices can be calculated with the quick algorithm of López-Sancho *et al.* [30] and Baquero [31], (see Refs. 22 and 23 for a compilation of the formulae and details of the algorithms used).

For any of the Green's functions given above the corresponding density of states, projected at a given layer, can be obtained from the usual formula

$$N(\mathbf{k}, \omega) = -\frac{1}{\pi} \text{Im} [\text{tr} G(\mathbf{k}, \omega)], \quad (4)$$

where \mathbf{k} is the 2D wave vector and ω is the energy eigenvalue. In the study of the (001) surface, for simplicity, we assume an ideal truncation. This approximation seems reasonable because it is widely accepted that the structural disorder effects in the ternary alloys are generally small [25, 33]. The total projected density of states is then obtained by integrating in the two-dimensional (2D) first Brillouin zone (BZ) using the method of Cunningham [34]. Here we have used a set of 9 special points in the BZ. For numerical convergence a small imaginary part of 0.001 eV to the real energy variable was added.

2.2. Our approach

In order to make this work self-contained we present here our treatment for the ternary alloys. Briefly speaking, we have used the tight-binding method and, under the conditions explained below, the VCA to study the ternary alloys. In this approach we take into account first nearest neighbor interactions, in the Slater-Koster language [14]. We use an orthogonal basis of five atomic orbitals (sp^3s^*) and, in our band structure calculations, we have included the effect of the spin-orbit interaction [17].

For the study of the ternary alloys we have included an *empirical bowing parameter* in the “s” on-site TBP of the substituted ion. This procedure give us the correct behaviour of the band gap as function of the composition. More exactly for the TBP of the ternary alloy we take their virtual crystal expression given by

$$\bar{E}_{\alpha,\alpha'}(x) = xE_{\alpha,\alpha'}^{(1)} + (1-x)E_{\alpha,\alpha'}^{(2)}, \quad \alpha, \alpha' = s, p^3, s^*, \quad (5)$$

for all but the “s” on-site TBP of the substituted ion. In Eq. 5 $E_{\alpha,\alpha'}^{(1,2)}$ are the TBP for the compound 1 (2); α, α' are the atomic orbitals used in the basis set.

For the “s” on-site TBP we use the following expression:

$$\bar{E}_{s,\nu}(x, b_\nu) = \bar{E}_{s,\nu}(x) + x(1-x)b_\nu, \quad \nu = a, c, \quad (6)$$

where $\bar{E}_{s,\nu}(x)$ is given by Eq. 5, and b_ν is an empirical bowing parameter per each different substitution. From Eq. 6 is clear that b_ν has energy units. This parameter could be thought as an *heuristic* description of the disorder effects. We can justify this approach by appealing to the simplicity of the treatment and the quality of the results, as we will show in the next section. The empirical bowing parameter used for the anion substitution in $\text{ZnSe}_{1-x}\text{Te}_x$ is $b_\nu = -6.964$ (complete and detailed treatment for other II-VI ternary alloys will be published elsewhere). With this Hamiltonians we can then calculate the band gap value and, of course, the electronic band structure for all the molar fraction in a straightforward way.

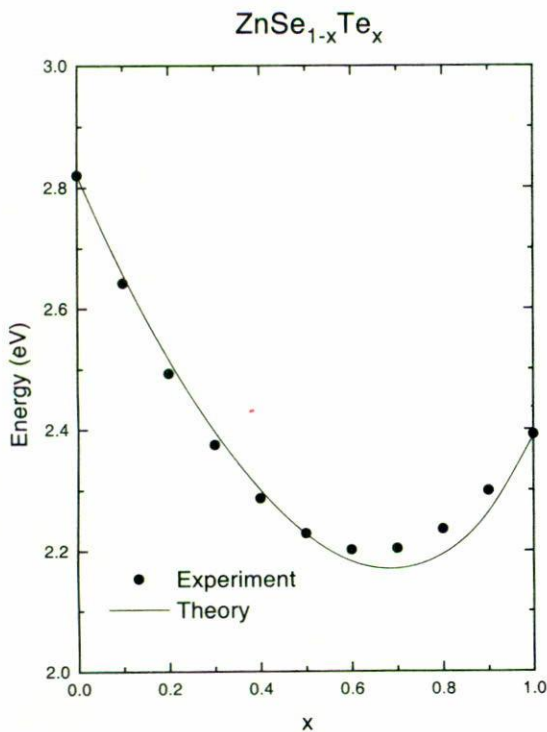


FIGURE 1. Band gap dependence on the molar fraction of $\text{ZnSe}_{1-x}\text{Te}_x$. The points are the experimental data of Ref. 33. The solid line shows the results of our calculation.

3. Results and discussion

3.1. The band gap calculation

Figure 1 shows our band gap calculation for the $\text{ZnSe}_{1-x}\text{Te}_x$ system. In the figure the experimental data are showed by points and the full line represents our calculation. The figure shows good agreement between the experimental and the theoretical curve, in particular in the $x < 0.5$ range. The experimental curve shows a minimum around $x_{\text{min}}^{\text{exp}} \approx 0.65$ which is very close to our calculated value $x_{\text{min}}^{\text{theo}} \approx 0.66$. At this x -value we obtain a band gap value of 2.47 eV, this is about 0.08 eV underestimated with respect to the experimental one [35]. We also have calculated the optical bowing parameter of the system and obtained the value of 1.51 eV, which is in good agreement with the experimental one, namely 1.507 ± 0.10 eV [35]. As is evident, our error is within the known accuracy of the method.

3.2. The electronic band structure

Within our approach, as explained in Sect. 2, we have calculated the electronic band structure for the case $x = 0.5$, and compared it with the extremal cases, namely, ZnSe ($x = 0$) and ZnTe ($x = 1$).

Figure 2 shows our electronic band structure calculation for this case. From this figure is clear that the calculated struc-

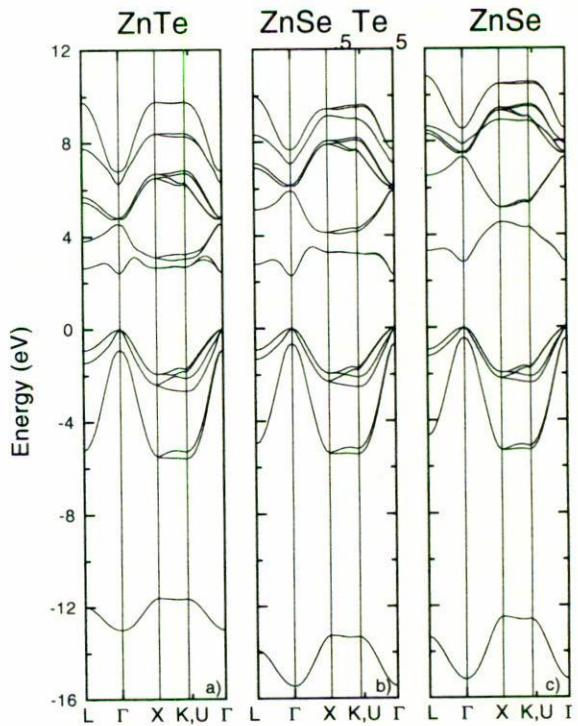


FIGURE 2. Electronic band structure for: a) ZnTe, b) $\text{ZnSe}_{0.5}\text{Te}_{0.5}$, and c) ZnSe. The electronic band structure for the ternary alloy has been calculated as explained in Section II B. The energy scale is referred to the maximum in the valence band.

ture, Fig. 2b, is representative of a semiconductor compound with a direct band gap. At the same time, Fig. 2b shows that in the upper valence band region it is very similar to the corresponding ZnTe case, see Fig. 2a. The lowest valence band resembles the ZnSe one, see Fig. 2c, but with energies values that are mixed between them.

In the conduction band region the lower conduction band is similar to the corresponding ZnTe one, as we have commented above, Sect. 3.1, for low Te-concentration. The rest of the bands are similar to the ZnSe case.

3.3. The LDOS calculation

Figure 3 shows our calculated bulk-projected LDOS for the $\text{ZnSe}_{1-x}\text{Te}_x$ alloy. We will concentrate our discussion only on the valence band region. Mainly, as is well known, because the tight-binding method gives a poor description for the upper conduction states.

We can observe in the figure the change of the bulk-projected LDOS going from ZnSe ($x = 0$) to ZnTe ($x = 1$). We obtain three peaks in the valence band region and four peaks in the conduction band region. The upper valence band width is ~ 5 and ~ 6 eV for ZnSe and ZnTe, respectively. For all the alloys we obtain an appropriate combination of these values, with exception of the $x = 0.6$ case. At this concentration we find a small upper valence band width. In this case we obtain a band width of about 3 eV. We should remind that

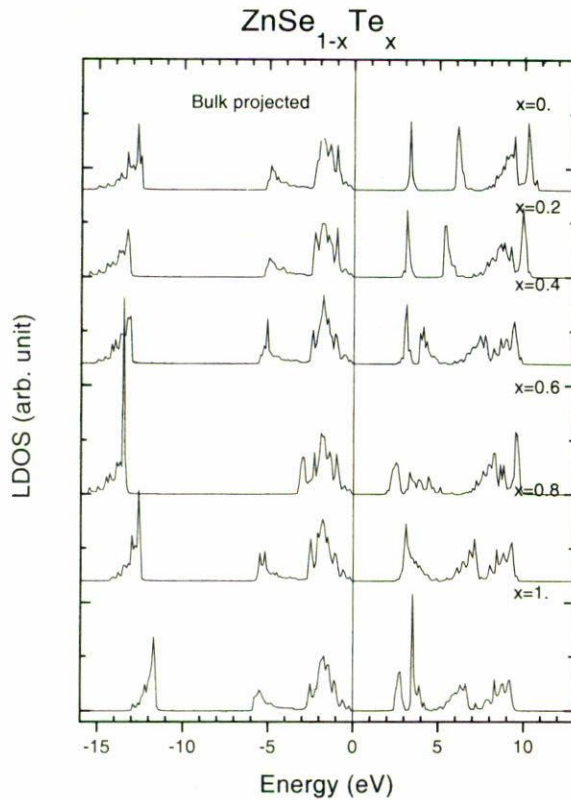


FIGURE 3. Bulk-projected local density of states for the (001)-surface for $\text{ZnSe}_{1-x}\text{Te}_x$. The calculation is showed at different x values.

this concentration corresponds to the minimum in the band gap value. At the same time, as we can see from the figure, we have a large increase of states in the bottom of the valence band. That is to say, the states “are moving” from the upper valence band states to the lower states. If we integrate the LDOS through out the valence band region, $\int N_{||}(\omega; x) d\omega$, we realize that the number of states in this case is the same that for the other x -values. As it should be expected: we have conservation of states for each different x -value, but we also get a redistribution of the electronic states.

In the lower valence band region, we find a wide gap in the valence band LDOS. This gap is ~ 7 and ~ 5.5 eV for ZnSe and ZnTe, respectively. We remark that these values are very close to the ones obtained in bulk, ~ 6 and ~ 5.4 for ZnSe and ZnTe, respectively [36, 37].

On the other hand, it is worth to comment that our LDOS shows almost the same pattern found by Li and Pötzt [24] using a large cluster approach, based on a tight-binding sp^3s^* model, within an *ab initio* calculation, or the molecular coherent pseudopotential approximation (MCPA) of Lempert *et al.* [25]. However, because our model is empirical and 2D in nature, we make no attempt to compete directly with more fundamental *a priori* approaches. We only show that our tight-binding and reformulated VCA approaches reproduce known features of the calculated density of states (DOS). In principle, we could think that in the calculation of the LDOS

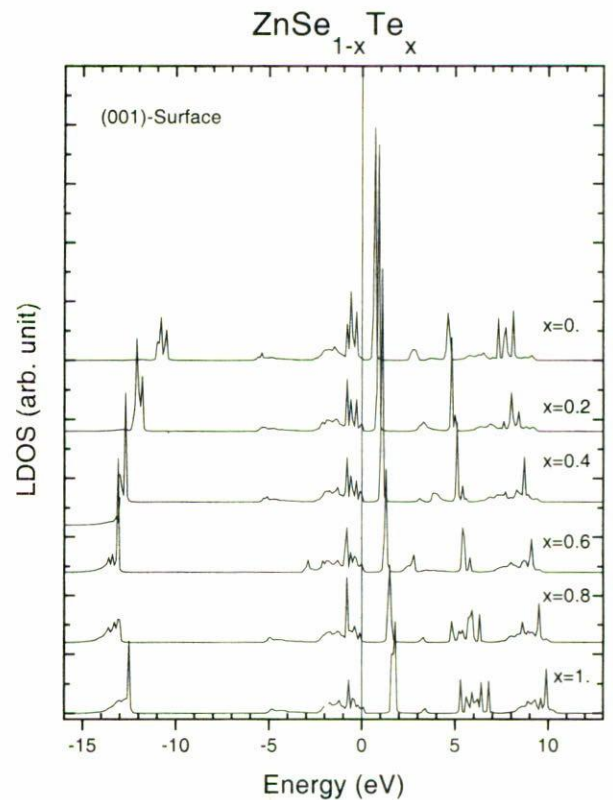


FIGURE 4. Local density of states projected on the first principal layer of the (001)-surface for $\text{ZnSe}_{1-x}\text{Te}_x$. The calculation is showed at different x values.

we should lose important information on the DOS, due to the losing of the Z -coordinate. However, in this work we are showing that the process lets us retain the main features of the DOS.

Finally, Fig. 4 shows our calculated LDOS projected onto the surface principal-layer. The main result, that can be observed from the figure, is the general narrowing of the band width. As is well established, this is mainly due to the loss of half of the first nearest neighbors for this surface [22]. Another peculiar result, showed in the figure, is the highly energy-localized surface state in the middle of the fundamental band gap for all concentrations, approximately. This fact was reported previously in the Ref. 32 for other II-VI binary compounds as well. At the same time we find a surface resonance near the top of the valence band. This surface resonance is characteristic of an anion terminated surface [21, 32]. (For a cation terminated surface, not showed in this calculation, there should appear a surface resonance in the middle of the valence band [21, 32]). A final resonance state is obtained in the bottom of the valence band, by looking at Figs. 3 and 4 we see that this resonance state moves together with the lowest bulk band as a function of x (see Ref. 21 for a detailed discussion of the valence band electronic structure of these and other II-VI semiconductor compounds).

4. Conclusions

In conclusion, we have shown that an adequate tight-binding description of the II-VI ternary alloys can be achieved within a reformulated virtual crystal approximation. This approach allow us to reproduce important properties of these systems, as the LDOS and surface states. Our confidence rests on the fact that we start from an adequate description of the bulk bands of the binary compounds. Our results are consistent with other more complicated calculations, and the method is not so expensive than these. In general, the valence band features, within our formulation, are in good agreement with the

molecular coherent pseudopotential approach calculations. We will show in the near future other useful applications of our approach.

Acknowledgments

This work was finished while the author was visiting the Max Planck Institut FKF in Stuttgart, Germany supported by the DAAD, the financial support is gratefully acknowledged. The author is indebted to Prof. V. Velasco and Dr. P. Vargas for their interest in this work, their stimulating commentaries, and critical reading of the manuscript.

1. G.W. Bryant, *Phys. Rev. Lett.* **55** (1985) 1786.
2. J.E. Lowther, *J. Phys. C: Solid State Phys.* **19** (1986) 1863.
3. D. Niles and H. Höchst, *Phys. Rev. B* **43** 1 (1991) 492.
4. K.U. Gawlik *et al.*, *Acta Physica Polonica A* **82** (1992) 355.
5. W. Bala, M. Drozdowski, and M. Kozielski, *Acta Physica Polonica A* **80** (1991) 723.
6. D.G. Kilday, G. Maragaritondo, T.F. Ciszek, and S.K. Deb, *J. Vac. Sci. Technol. B* **6** (1988) 1364.
7. T.M. Duc, C. Hsu, and J.P. Faurie, *Phys. Rev. Lett.* **58** (1987) 1127.
8. J. Arriaga and V.R. Velasco, *Physica Scripta* **46** (1992) 83.
9. M.J.S.P. Brasil *et al.*, *Appl. Phys. Lett.* **59** 1 (1991) 206.
10. Y.P. Feng *et al.*, *J. Appl. Phys.* **74** (1993) 3948.
11. K. Ichino *et al.*, *J. Electronic Mat.* **22** (1993) 445.
12. D. Olguín, R. de Coss, and R. Baquero, (unpublished).
13. E. García, A. Camacho, D. Olguín, and R. Baquero, (unpublished).
14. J.C. Slater and G.F. Koster, *Phys. Rev.* **94** (1954) 1498.
15. P. Volg, H.P. Hjalmarson, and J.D. Dow, *J. Phys. Chem. Solids* **44** (1983) 365.
16. W.A. Harrison, *Phys. Rev. B* **24** (1981) 5835.
17. J.D. Chadi, *Phys. Rev. B* **16** (1977) 790.
18. C. Priester, D. Bertho, and C. Jouanin, *Physica B* **191** (1993) 1.
19. D. Olguín and R. Baquero, *Phys. Rev. B* **50** (1994) 980.
20. F. García-Moliner and V. Velasco, *Theory of Single and Multiple Interfaces*, (World Scientific, Singapore, 1992); F. García-Moliner and V.R. Velasco, *Prog. Surf. Sci.* **21** (1986) 93.
21. D. Olguín and R. Baquero, *Phys. Rev. B* **51** (1995) 981.
22. R. Baquero and A. Noguera, *Rev. Mex. Fís.* **35** (1987) 638.
23. C. Quintanar, R. Baquero, F. García-Moliner, and V.R. Velasco, *Rev. Mex. Fís.* **37** (1991) 503.
24. Z.Q. Li and W. Pötz, *Phys. Rev. B* **46** (1992) 2109.
25. R.J. Lempert, K.C. Hass, and H. Ehrenreich, *Phys. Rev. B* **36** (1987) 1111.
26. S. Vlaev, V. Velasco, and F. García-Moliner, *Phys. Rev. Lett.* **49** 11 (1994) 222.
27. S. Vlaev, V. Velasco, and F. García-Moliner, *Phys. Rev. Lett.* **50** (1994) 4577; **51** (1995) 7321; **52** 13 (1995) 784; S. Vlaev and D.A. Contreras, *J. Appl. Phys.* **82** (1997) 3853.
28. R. Baquero, V.R. Velasco, and F. García-Moliner, *Physica Scripta* **38** (1988) 742.
29. L. Falicov and F. Yndurain, *J. Phys. C: Solid St. Phys.* **8** (1975) 147.
30. M.P. López-Sancho, J.M. López-Sancho, and J. Rubio, *J. Phys. F: Metal Phys.* **14,15** (1984,85) 1205, 855.
31. R. Baquero, (unpublished).
32. F. Rodríguez, A. Camacho, L. Quiroga, and R. Baquero, *Phys. Status Solidi* **160** (1990) 127.
33. K.L. Tsang, J.E. Rowe, T.A. Callcott, and R.A. Logan, *Phys. Rev. B* **38** 13 (1988) 277.
34. S.L. Cunningham, *Phys. Rev. B* **10** (1974) 4988.
35. M.J.S.P. Brasil *et al.*, *Appl. Phys. Lett.* **58** (1991) 2509.
36. J.R. Chelikowsky, T.J. Wagener, J.H. Weaver, and A. Jin, *Phys. Rev. Lett.* **40** (1989) 9644; J.R. Chelikowsky and M.L. Cohen, *Phys. Rev. Lett.* **16** 1976 556.
37. We have obtained the DOS-values for ZnTe from a LMTO-ASA calculation performed by P. Vargas from Max Planck Institut-Stuttgart, Germany.